The Journal of Immunology

Osteal Tissue Macrophages Are Intercalated throughout Human and Mouse Bone Lining Tissues and Regulate Osteoblast Function In Vitro and In Vivo

Ming K. Chang, Liza-Jane Raggatt, Kylie A. Alexander, Julia S. Kuliwaba, Nicola L. Fazzalari, Kate Schroder, Erin R. Maylin, Vera M. Ripoll, David A. Hume and Allison R. Pettit

J Immunol 2008; 181:1232-1244; ;
doi: 10.4049/jimmunol.181.2.1232
http://www.jimmunol.org/content/181/2/1232

The Journal of Immunology is published twice each month by
The American Association of Immunologists, Inc.,
1451 Rockville Pike, Suite 650, Rockville, MD 20852

Print ISSN: 0022-1767 Online ISSN: 1550-6606.

Osteal Tissue Macrophages Are Intercalated throughout Human and Mouse Bone Lining Tissues and Regulate Osteoblast Function In Vitro and In Vivo[1]

Ming K. Chang,[2]* Liza-Jane Raggatt,[2]* Kylie A. Alexander,* Julia S. Kuliwaba,† Nicola L. Fazzalari,† Kate Schroder,* Erin R. Maylin,* Vera M. Ripoll,*‡ David A. Hume,*§ and Allison R. Pettit[3]*

Resident macrophages are an integral component of many tissues and are important in homeostasis and repair. This study examines the contribution of resident tissue macrophages to bone physiology. Using immunohistochemistry, we showed that a discrete population of resident macrophages, OsteoMacs, was intercalated throughout murine and human osteal tissues. OsteoMacs were distributed among other bone lining cells within both endosteum and periosteum. Furthermore, OsteoMacs were coisolated with osteoblasts in murine bone explant and calvarial preparations. OsteoMacs made up 15.9% of calvarial preparations and persisted throughout standard osteoblast differentiation cultures. Contrary to previous studies, we showed that it was OsteoMacs and not osteoblasts within these preparations that responded to pathophysiological concentrations of LPS by secreting TNF. Removal of OsteoMacs from calvarial cultures significantly decreased osteocalcin mRNA induction and osteoblast mineralization in vitro. In a Transwell coculture system of enriched osteoblasts and macrophages, we demonstrated that macrophages were required for efficient osteoblast mineralization in response to the physiological remodeling stimulus, elevated extracellular calcium. Notably, OsteoMacs were closely associated with areas of bone modeling in situ, forming a distinctive canopy structure covering >75% of mature osteoblasts on diaphyseal endosteal surfaces in young growing mice. Depletion of OsteoMacs in vivo using the macrophage-Fas-induced apoptosis (MAFIA) mouse caused complete loss of osteoblast bone-forming surface at this modeling site. Overall, we have demonstrated that OsteoMacs are an integral component of bone tissues and play a novel role in bone homeostasis through regulating osteoblast function. These observations implicate OsteoMacs, in addition to osteoclasts and osteoblasts, as principal participants in bone dynamics. ***The Journal of Immunology,*** **2008, 181: 1232–1244.**

Calcium and bone homeostasis require a precise coupled balance between the opposing activities of cells that produce calcified bone matrix (osteoblasts) and those that degrade it (osteoclasts). Osteoblasts are mesenchymal bone-forming cells that undergo sequential differentiation, ultimately giving rise to mature cells that produce and mineralize bone matrix (1). The molecular and cellular mechanisms driving osteoblast differentiation and mineralization in vivo are incompletely understood and this deficiency is translated to our limited ability to clinically manipulate bone formation.

Several lines of evidence motivated us to investigate the potential contribution of macrophages to bone physiology. First, macrophages are closely related to bone-resorbing osteoclasts and share a dependence on the lineage-specific growth factor CSF-1 (2). Although inflammatory macrophages are well acknowledged for their roles in immunity and chronic inflammation, it is less widely recognized that there are populations of resident tissue macrophages present in most tissues throughout development and adulthood (e.g., alveolar macrophages and Kupffer cells (3)). These resident macrophages undergo tissue-specific adaptation and contribute to ongoing physiological processes and tissue repair (4). Murine tissue macrophages are routinely identified using the F4/80 Ag that is expressed by most mature tissue macrophages but not other closely related cells, including osteoclasts (5). F4/80$^+$ macrophages have been found to be associated with bone surfaces (6), but their frequency, distribution, and tissue-specific functional contributions have not been explored. Given the key roles of macrophages in other tissues, including trophic functions (7), their presence in osteal tissues raises the question of whether macrophages are a third player in bone homeostasis and turnover.

Second, osteoblasts have been extensively studied using primary cells isolated from neonatal rodent calvaria (8) that are differentiated in vitro using a combination of ascorbic acid and β-glycerophosphate (9). Calvarial osteoblast preparations are morphologically heterogeneous (10), but their reported phenotypes and functions are generally attributed to the osteoblast component of

*Institute for Molecular Bioscience, Cooperative Research Centre for Chronic Inflammatory Diseases, University of Queensland, Brisbane, Queensland, Australia; †Institute of Medical and Veterinary Science and Hanson Institute, Adelaide, South Australia, Australia; ‡Medical Research Council, Mammalian Genetics Unit, Harwell, United Kingdom; and §Roslin Institute and Royal (Dick) School of Veterinary Studies, University of Edinburgh, Roslin, United Kingdom

Received for publication March 19, 2008. Accepted for publication May 14, 2008.

The costs of publication of this article were defrayed in part by the payment of page charges. This article must therefore be hereby marked *advertisement* in accordance with 18 U.S.C. Section 1734 solely to indicate this fact.

[1] This work was supported by National Health and Medical Research Council (Grant 455941); Ramaciotti Foundations (Grant RA078/05); and University of Queensland Early Career Grant (Project 2004001479). The following authors received funding from National Health and Medical Research Council: M.K.C., Dora Lush Scholarship (Grant ID 409913); K.A.A., Dora Lush Scholarship (Grant ID 409914); and L.-J.R., Peter Doherty Fellowship (Grant ID 252934).

[2] M.K.C and L.J.R contributed equally to this work.

[3] Address correspondence and reprint requests to Dr. Allison R. Pettit, Institute for Molecular Bioscience, University of Queensland, Brisbane, Queensland 4072, Australia. E-mail address: a.pettit@imb.uq.edu.au

Table I. *Sequence of primers used in real-time RT-PCR*

Gene	Accession No.	Forward Primer (5′–3′)	Reverse Primer (5′–3′)
hprt	NM_013556.2	GCAGTACAGCCCCAAAATGG	AACAAAGTCTGGCCTGTATCCAA
col1a1	NM_007742.3	GGTCCTCGTGGTGCTGCT	ACCTTTGCCCCCTTCTTTG
alp	NM_007431	GATAACGAGATGCCACCAGAGG	TCCACGTCGGTTCTGTTCTTC
oc	NM_007541.2	GAGGGCAATAAGGTAGTGAACAGA	AAGCCATACTGGTTTGATAGCTCG
emr1	NM_01013.3	CTCTGTGGTCCCACCTTCAT	GATGGCCAAGGATCTGAAAA
csf1r	NM_001037859.2	CCACCATCCACTTGTATGTCAAAGAT	CTCAACCACTGTCACCTCCTGT
tlr4	NM_021297.2	TGGCTAGGACTCTGATCATGGC	TGAAGAAGGAATGTCATCAGGG
md-2	NM_016923.1	TGCATGTTGAGTTCATTCCAA	GGCACAGAACTTCCTTACGC
cd14	NM_009841.3	CAGAATCTACCGACCATGGAG	GGAACAACTTTCCTCGTCTAGC 1

Hprt, hypoxanthine-guanine phosphoribosyl transferase; *col1a1,* collagen type I; *alp,* tissue nonspecific alkaline phosphatase; *oc,* osteocalcin; *emr1, f4*/80; *csf1r,* CSF- 1R, and *tlr4,* TLR4.

these cell preparations. This includes macrophage-related functions such as phagocytosis (11), detection of bacterial products (12), and Ag presentation (11). As studies of long-term primary cultures from ovary have been demonstrated to contain a self-replicating monocyte-macrophage population (13), and macrophages are located within the bone microenvironment (6), we considered the possibility that macrophages are coisolated and maintained in primary osteoblast cultures.

In this study, we systematically analyzed the presence and distribution of macrophages on mouse and human bone surfaces in situ and their presence in primary calvarial osteoblast preparations. We also investigated the possibility that macrophages, and not osteoblasts, are the cells within primary osteoblast cultures that respond to the bacterial product LPS. Finally, we tested the ability of macrophages to influence osteoblast differentiation and mineralization in vitro and in vivo. Taken together, the data indicate that macrophages are key participants, alongside osteoclasts and osteoblasts, in bone homeostasis and dynamics.

Materials and Methods

Animals

C57BL/6 and MacGreen mice (14), backcrossed for six generations to the C57BL/6 background, were maintained in a specific pathogen-free facility. MAFIA-transgenic mice were a generous gift from Prof. D. Cohen (Department of Microbiology, Immunology and Molecular Genetics, University of Kentucky, Lexington, KY) and were maintained in a quarantine facility. The University of Queensland Molecular Biosciences Ethics Committee approved all animal protocols.

Tissue collection

For murine tissues, 4-wk-old C57BL/6 left hind limbs were dissected, extraneous soft tissue was removed before overnight fixation in 4% paraformaldehyde (PFA)[4] at 4°C and subsequently decalcified for 2 wk in 14% EDTA (pH 7.2). For human tissues, a 10-mm tube saw bone biopsy was obtained from the intertrochanteric region of the proximal femur, distal to the active site of disease, from 12 individuals undergoing total hip arthroplasty surgery for primary osteoarthritis (OA). Tissues were collected from six male and six female donors, with a median age of 65.5 years. Ethical approval was obtained from both the University of Queensland Medical Research Ethics Committee and Research Ethics Committee Royal Adelaide Hospital. Fresh surgical intertrochanteric bone specimens were fixed in 4% PFA overnight at 4°C and decalcified in 15% EDTA/4% PFA for up to 4 wk. Radiography was used to monitor the decalcification process. Once decalcified, all specimens were processed for paraffin embedding and 5-μm sections were cut on a rotary microtome and placed on SuperFrost Plus or Ultra Plus slides (Menzel-Glaser).

Immunohistochemistry and immunocytochemistry

In mouse tissues, expression of F4/80 (rat anti-mouse; AbD Serotec), collagen type I (rabbit anti-mouse; U.S. Biological) and osteocalcin (rabbit anti-mouse; Alexis Biochemicals) were examined in serial sections. Anti-CD68 (mouse anti-human; DakoCytomation) staining was performed in human tissues. Sections were deparaffinized and rehydrated followed by Ag retrieval. This was achieved in mouse tissues using 0.37% trypsin (Biocare Medical) for 10 min and in human tissues using heat retrieval in 10 mM EDTA (pH 7.5). Cells grown on chamber slides were fixed with 4% PFA for 30 min. Immunostaining was performed using an immunoperoxidase technique with diaminobenzidine (DakoCytomation) as the chromogen. TBS was used for dilutions and washes between each step. Briefly, sections were incubated in serum block for 60 min (10% FCS (Invitrogen) plus 10% normal goat serum or 10% normal rabbit serum (AbD Serotec)), followed by specific primary Ab or isotype-matched control Ab (60 min). Each of the following incubations were for 30 min. Endogenous peroxidase activity was blocked using 3% H_2O_2. Sections were subsequently incubated with a biotinylated $F(ab')_2$ of species-matched secondary Ab: goat anti-rat, goat anti-rabbit (Santa Cruz Biotechnology) or rabbit anti-mouse (DakoCytomation) Ig followed by HRP-conjugated streptavidin (DakoCytomation). Diaminobenzidine was developed as per the manufacturer's instructions and all sections were counterstained with Mayer's hematoxylin (Sigma-Aldrich) and mounted using permanent mounting medium. Sections were examined using an Olympus BX-51 microscope with a DP-70 digital camera and DP controller imaging software (Olympus).

Confocal and epifluorescent microscopy imaging of osteal tissues

Visualization of endosteal macrophages was performed by confocal microscopy (Zeiss META inverted confocal microscope and LSM 510 software, version 3.2; Zeiss Germany) on cultured bone fragments collected from MacGreen mice. Bone fragments were fixed with 4% PFA and blocked in 5% FBS before incubation with anti-F4/80 Ab or isotype control rat IgG2b (AbD Serotec) followed by species-matched Alexa Fluor 594-conjugated secondary Ab (Molecular Probes and Invitrogen). Cells were permeabilized using Triton X-100 and nuclei were stained using DAPI (Roche Diagnostics). Results were examined by confocal microscopy. Visualization of periosteal macrophages was achieved by epifluorescent microscopy on MacGreen neonatal calvaria. The calvaria were dissected, fixed using 4% PFA, counterstained with DAPI, and visualized using an Olympus BX-51 epifluorescence light microscope with a DP-70 digital camera and DP controller imaging software (Olympus).

Isolation, differentiation, and enrichment of primary osteoblasts

Primary osteoblast cells were isolated by 10-min sequential digestion of 2-day-old neonatal C57BL/6 calvaria with 0.25 U/ml collagenase D (Roche Diagnostics) and 2.2 U/ml dispase (Invitrogen). Digest fractions 2–6 were pooled as unsorted calvarial osteoblasts. These cells were enriched with MACS technology using a mature hematopoietic lineage cell depletion kit supplemented with mouse CD11b microbeads (Miltenyi Biotec) according to the manufacturer's instructions. The depleted cells were also collected (termed bone macrophages) and the number of $F4/80^+$ cells was determined by flow cytometry. Osteoblasts were cultured in complete MEM supplemented with 10% heat-inactivated FBS, 20 U/ml penicillin, 20 μg/ml streptomycin, and 2 mM L-glutamine (Invitrogen). In brief, 1.38×10^4 or 6.9×10^4 unsorted osteoblasts and 1.2×10^4 or 6×10^4 enriched osteoblasts were seeded (seeding numbers adjusted to ensure equal seeding of osteoblasts in unsorted and enriched cultures) per well in 4-well chamber slides (Corning Life Sciences) or 6-well plates (Nunc), respectively. Osteoblasts were differentiated in complete BGJb medium (Invitrogen) with 50 μg/ml ascorbic acid (Sigma-Aldrich) and 10 mM β-glycerophosphate (Sigma-Aldrich) from day 7 of culture.

[4] Abbreviations used in this paper: PFA, paraformaldehyde; OA, osteoarthritic; DAPI, 4′,6-diamidino-2-phenylindole; BMM, bone marrow-derived macrophage; ObS, osteoblast bone surface; eGFP, enhanced GFP; TRAP, tartate-resistant acid phosphatase; MAFIA, macrophage-Fas-induced apoptosis.

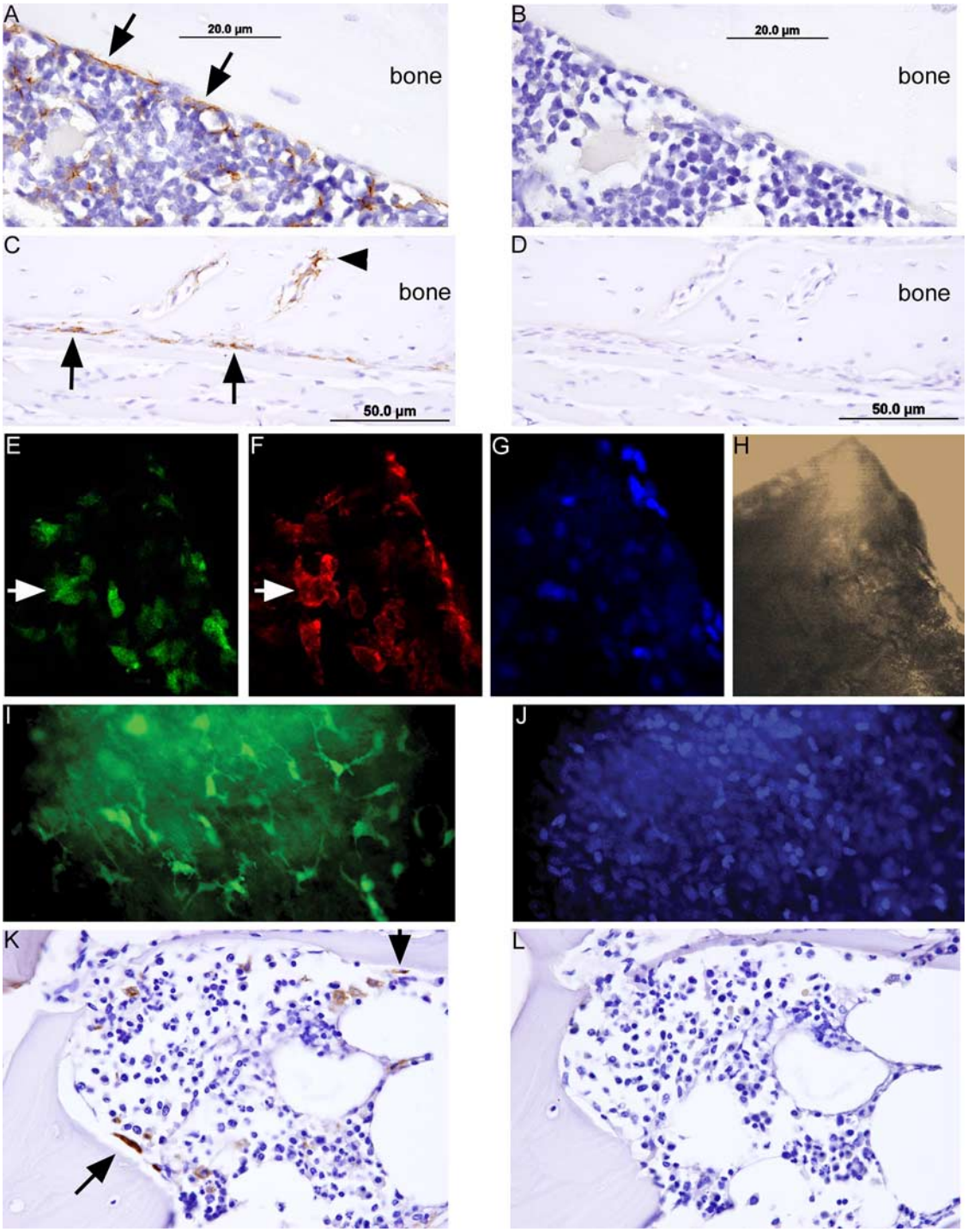

FIGURE 1. Macrophages are intercalated throughout resting endosteal and periosteal bone surfaces. *A–D,* Immunohistochemical staining in sagittal cross-sections of 4-wk-old mouse cortical long bone in the diaphyseal region. Sections were counterstained with hematoxylin (blue). F4/80$^+$ macrophages (brown staining) were located immediately adjacent to resting endosteal (*A*, arrows) and periosteal (*C*, arrows) bone surfaces. F4/80$^+$ macrophages were also present in endosteum lining blood vessel channels (*C*, arrowhead). *B* and *D,* The specificity of staining was confirmed using the relevant isotype control Ab in a serial section. Bone matrix is identified as "bone." *E–H,* More detailed visualization and confirmation of macrophage phenotype was achieved using confocal microscopy of MacGreen endosteal bone surface stained with anti-F4/80 Ab (red) and the nuclear stain DAPI (blue). *E,* Large eGFP$^+$ cells with macrophage morphology were detected on the endosteal surface. *F,* These eGFP$^+$ cells coexpressed F4/80 (example indicated by arrow in both *E* and *F*). *G,* DAPI staining demonstrated that the macrophages were intercalated among other cells on the endosteal surface. *H,* Transmitted light imaging was used to visualize the bone fragment in *E–G*. *I* and *J,* Epifluorescent microscopy of MacGreen neonatal calvaria. Stellate eGFP$^+$ macrophages were distributed throughout the periosteum (*I*), intercalated among other periosteal cells as indicated by DAPI nuclear staining (*J*). *K* and *L,* Macrophages were identified using immunohistochemical staining in OA human bone sections counterstained with hematoxylin (blue). *K,* CD68 staining (brown) identified macrophage-like cells both immediately adjacent to bone (arrows and arrowhead) and within the bone microenvironment. *L,* The specificity of staining was confirmed using the relevant isotype control Ab in a serial section. Original magnifications: ×100 (*A* and *B*), ×63 (*E–H*), ×60 (*K* and *L*), and ×40 (*C, D, I,* and *J*).

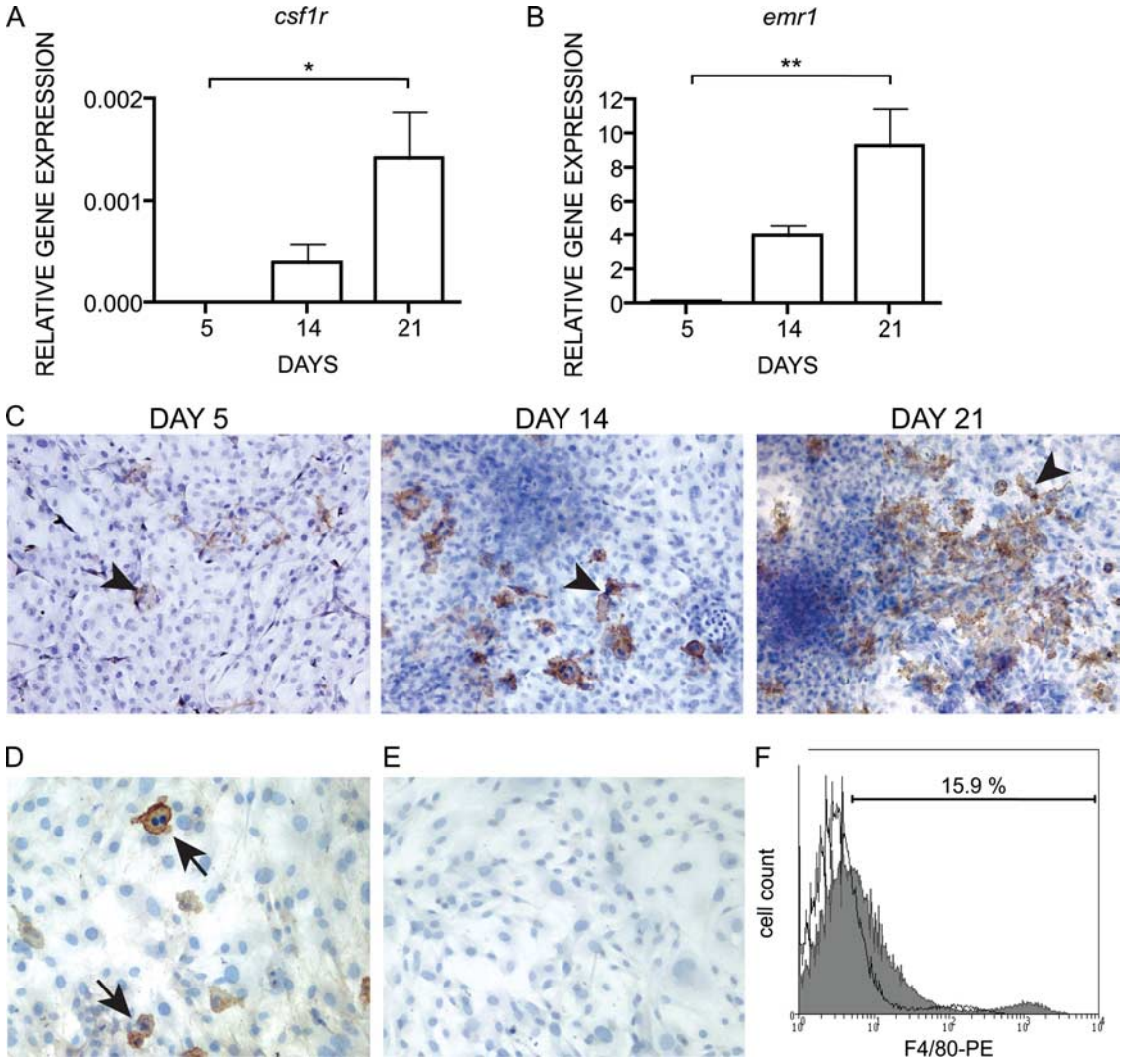

FIGURE 2. Macrophages are coisolated in primary calvarial osteoblast cultures. Quantitative RT-PCR analysis validated the expression of the macrophage marker genes *csf1r* (*A*) and *emr1* (*B*) in primary osteoblast preparations over a standard differentiation time course. Data are mean ± SEM of three independent experiments. Statistically significant differences (*, $p < 0.05$ and **, $p < 0.01$) were determined by one-way ANOVA. *C,* The presence of F4/80$^+$ macrophages (brown, arrowheads) within osteoblast cultures over the differentiation time course was assessed by immunocytochemical staining. F4/80$^+$ cells undergoing mitotic cell division were detected (*D*, arrows). *E,* Isotype-matched control staining was used to confirmed Ab specificity. Samples were counterstained with hematoxylin. Original magnification, ×10. *F,* Flow cytometric analysis of F4/80 expression (filled histogram) or isotype control (open histogram) in calvarial digest cells. All data are representative of three independent experiments.

RNA isolation and quantitative real time RT-PCR

Total RNA was isolated, reverse transcribed, and analyzed using quantitative real time RT-PCR as previously described (15). The sequences of primers used are described in Table I.

Flow cytometric analysis

Calvarial osteoblast cells (5×10^5) were blocked in 0.5% FBS/PBS before incubation with either FITC- or PE- conjugated anti-F4/80 Ab (AbD Serotec) or relevant isotype rat IgG2b (AbD Serotec). Cells were then fixed with 4% PFA and examined by flow cytometry on a BD LSR II Analyzer (BD Biosciences). Data was analyzed using the Weasel software (Walter and Eliza Hall Institute of Medical Research, Melbourne, Australia).

LPS stimulation of calvarial osteoblast cultures

Unsorted and enriched calvarial osteoblasts grown on chamber slides were stimulated with 100 ng/ml LPS (*Salmonella minnesota*; Sigma-Aldrich) for 2 h at days 14 and 21 of differentiation culture. Culture medium was collected from LPS-treated explant cultures and calvarial osteoblast cultures (at days 14 and 21). Secreted TNF protein was detected using a BD Pharmingen OptEIA mouse TNF ELISA kit II according to the manufacturer's instructions.

Coculture of enriched osteoblasts with macrophages

BMMs were differentiated from C57BL/6 bone marrow progenitors as previously described (15). Enriched calvarial osteoblasts (1.2×10^4) were cocultured with macrophages (1.8×10^3; bone macrophages or BMMs) using 24-Transwell plates with 0.4-μm pore size (Corning Life Sciences). Osteoblasts were seeded on the bottom of the wells and macrophages were seeded on the inserts. Cells were cultured in complete MEM with 14 mM $CaCl_2$ or 1 M HEPES vehicle control (Thermo Electron) for 14 days.

Assessment of osteoblast mineralization by von Kossa staining

Cells were fixed with 4% PFA. For von Kossa staining, cells were stained with 1% silver nitrate (Sigma-Aldrich) while exposed to UV light and then incubated with 5% sodium thiosulfate (AJAX Finechem). Chamber slide wells from standard osteoblast differentiation assays were photographed using a transmitted light microscope (BX-51) with a DP-70 digital camera and DP controller imaging software (Olympus). Twenty-four-well plates from extracellular calcium stimulated coculture assays were imaged using a BD Biosciences Pathway Bioimager. The area of mineralization (black precipitate) in each well was quantified using NIH ImageJ software and is represented as the percentage of total area analyzed.

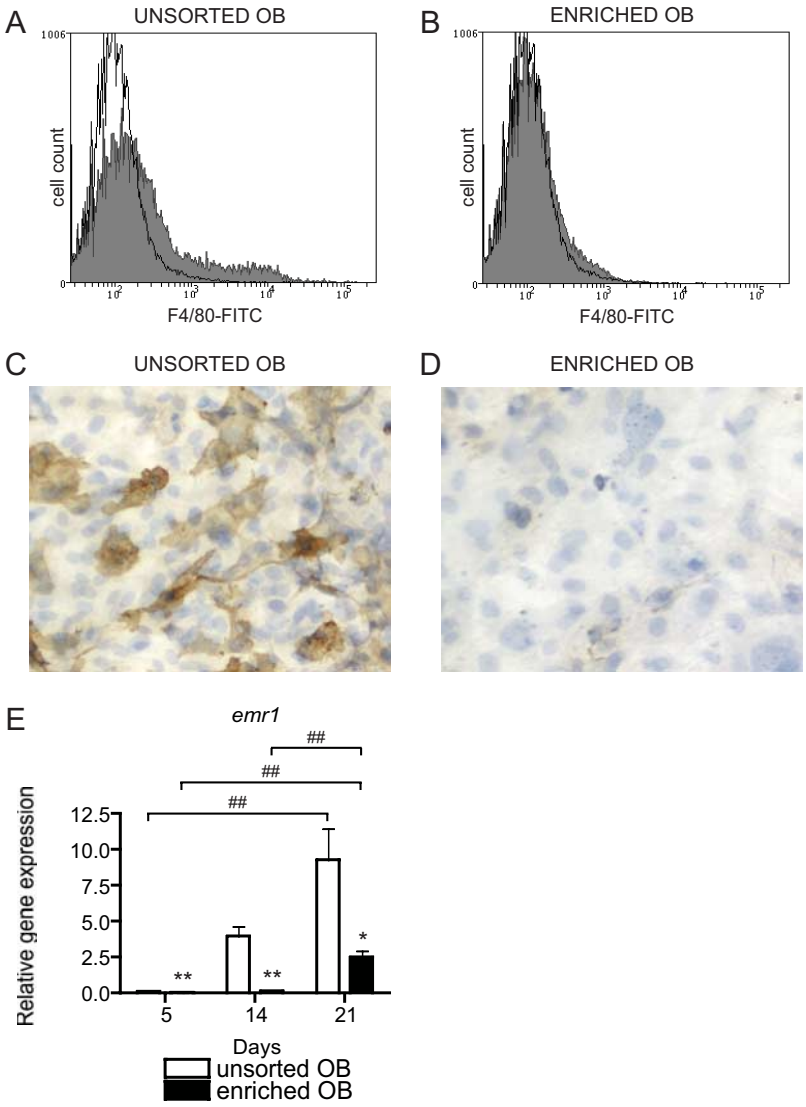

FIGURE 3. Enrichment of primary osteoblasts. Unsorted calvarial digest cells (*A*) and the enriched osteoblast population (*B*) were analyzed by flow cytometry to confirm depletion of F4/80$^+$ macrophages (anti-F4/80 Ab, filled histogram and isotype control, open histogram). Data are representative of three independent experiments. Immunocytochemistry staining for F4/80 expression in unsorted osteoblasts (*C*) and enriched osteoblast culture (*D*) at day 21. Original magnification, ×10. Data are representative of three independent experiments. Real-time RT-PCR quantified the expression of the macrophage marker gene *emr1* (*E*) in unsorted and enriched osteoblast populations over a differentiation time course. Data are mean ± SEM of three independent experiments. Statistical significance between populations (*, $p < 0.05$ and **, $p < 0.01$) was determined by an unpaired *t* test; whole significance across the time course was calculated using one-way ANOVA (##, $p < 0.01$). OB, Osteoblast.

Adapted histomorphometry

The F4/80$^+$ cell canopy structure was quantified by adapting standard histomorphometry. Analysis was performed in 5-μm sections of long bones from 4-wk-old animals ($n = 7$) stained for F4/80 expression. Three independent measurements were performed in each sample at least 50 μm apart. Serial images were collected of the endosteal bone surface extending from the base of the metaphyseal growth plate and through the diaphyseal zone and tiled together (average of 47 mm of bone surface analyzed per sample). The identity of mature osteoblasts was confirmed in serial sections stained with anti-collagen type I and anti-osteocalcin Abs. Total osteoblast bone surface (ObS; average of 63 ± 5.7%) and the amount of ObS covered by F4/80$^+$ OsteoMac canopy were determined using ImageJ software.

Depletion of macrophages using the MAFIA-transgenic mouse model

Macrophages were depleted using an 8-day i.v. injection regimen of either 10 mg/kg AP20187 ($n = 7$, generous gift from ARIAD Pharmaceuticals) or vehicle control ($n = 7$) in 8-wk-old MAFIA-transgenic mice, as previously described (16). Hind limb bones were harvested, processed for paraffin embedding, stained for collagen type I or F4/80 expression using immunohistochemistry, and analyzed by adapted histomorphometry, as described above, but at only one section depth. Bone marrow was also collected from the contralateral limb of all animals at the time of tissue harvest. Flow cytometric analysis on individual bone marrow cell suspension, performed as described above was used to confirm F4/80$^+$ macrophage depletion in bone marrow.

Statistical analysis

Statistically significant differences were determined using one-way ANOVA, paired *t* test, or unpaired *t* test with two-tailed distributions where appropriate using PRISM 4 (GraphPad software). A value of $p < 0.05$ was deemed statistically significant. In all cases, data are represented as mean ± SEM.

Results

Macrophages are intercalated throughout osteal tissues

Bone is lined by specialized osteal tissues: the periosteum on the outer surface and the endosteum on the internal surface in direct contact with the marrow (17). Endosteum, in its resting state, is one to two cells thick and predominantly consists of "bone lining" cells that are thought to be immature/quiescent osteoblasts. The periosteum is relatively more complex and, in addition to bone lining cells, includes a capsule layer, blood vessels, and nerves. Cells within the endosteum and periosteum are responsible for maintaining/regulating bone integrity, growth, and mineral homeostasis (17). Immunohistochemical staining for F4/80 protein expression in sagittal sections of murine long bone demonstrated the presence of numerous F4/80$^+$ mature tissue macrophages distributed throughout cortical endosteal (Fig. 1*A*, arrows) and periosteal tissues (Fig. 1*C*, arrows), as well as bone lining tissues of

trabecular bone (data not shown). F4/80$^+$ macrophages were also commonly observed in the perivascular region of blood vessel channels within bone (Fig. 1*C*, arrowhead). Confocal microscopy assessment of bone surfaces collected from MacGreen mice (in which the *csf1r* promoter drives the expression of the enhanced GFP (eGFP), resulting in eGFP$^+$ macrophages and other myeloid cells (14)), showed coexpression of eGFP and the F4/80 Ag within the endosteum (Fig. 1, *E* and *F*, arrows), verifying the presence of mature macrophages within this tissue. Nuclear staining with 4′,6-diamidino-2-phenylindole (DAPI) demonstrated that the macrophages are intercalated among other bone lining cells (Fig. 1*G*). Confocal z-stack scanning analysis confirmed that the eGFP$^+$ cells followed the concave contour of the endosteal bone surface (data not shown), supporting that the macrophages are indeed located within the bone lining tissue. Similarly, en face epifluorescent microscopy of neonatal calvaria demonstrated stellate F4/80$^+$ macrophages distributed throughout the periosteum (Fig. 1*I*). Again, DAPI nuclear staining indicated that these macrophages are intercalated among other periosteal cells (Fig. 1*J*). These observations demonstrate that mature tissue macrophages, which we will refer to as OsteoMacs (in line with the osteoclast and osteoblast nomenclature), reside within and are distributed throughout osteal tissues.

We next investigated whether OsteoMacs were present within human osteal tissue. This was achieved using immunohistochemistry staining for the macrophage marker CD68 (lysosomal-associated transmembrane glycoprotein highly expressed by human tissue macrophages (18)) in human trabecular bone samples from OA patients. CD68$^+$ macrophage-like cells were observed both immediately adjacent to bone (Fig. 1*K*, arrows and arrowhead) and within the bone microenvironment (Fig. 1*K*). These results support that OsteoMacs are an integral component of mouse and human osteal tissues.

Macrophage-restricted genes are expressed in primary osteoblast cultures

Primary osteoblasts have been routinely harvested from neonatal rodent calvaria (8) and differentiated in vitro. Primary mouse calvarial osteoblasts were analyzed for gene expression at three key stages of osteoblast growth: proliferation (day 5), differentiation (day 14), and mineralization (day 21). Well-characterized markers of osteoblast functional differentiation (alkaline phosphatase NM_007431, collagen type I NM_007742.3, and osteocalcin NM_007541.2) were expressed and up-regulated in a temporal order (data not shown), confirming that our culture conditions recapitulate in vitro osteoblast differentiation as reported by others (1). Initial analysis of these RNA samples by microarray, as part of the Novartis Symatlas project (analyzed a large panel of tissues and cell lineages using the Affymetrix platform, http://symatlas.gnf.org/SymAtlas/, see the D.Hume dataset or Gene Expression Omnibus (GEO) experiment 11339 (http://www.ncbi.nlm.nih.gov/projects/geo/)) (19), surprisingly showed that osteoblast cultures expressed many genes that are normally specifically transcribed in macrophages. Notably, osteoclast-associated genes were minimally expressed in these cultures, including tartrate-resistant acid phosphatase (TRAP) and calcitonin receptor (data available at http://symatlas.gnf.org/SymAtlas/and GEO experiment 11339) and TRAP$^+$ osteoclasts did not form in these cultures (data not shown). The expression of macrophage genes in primary osteoblast cultures was validated by quantitative RT-PCR for the macrophage-restricted mRNAs *csf1r* (NM_001037859.2) and *emr1* (*f4/80;* NM_010130.3) (20). Both *csf1r* and *emr1* were expressed in primary osteoblast cultures (Fig. 2, *A* and *B*).

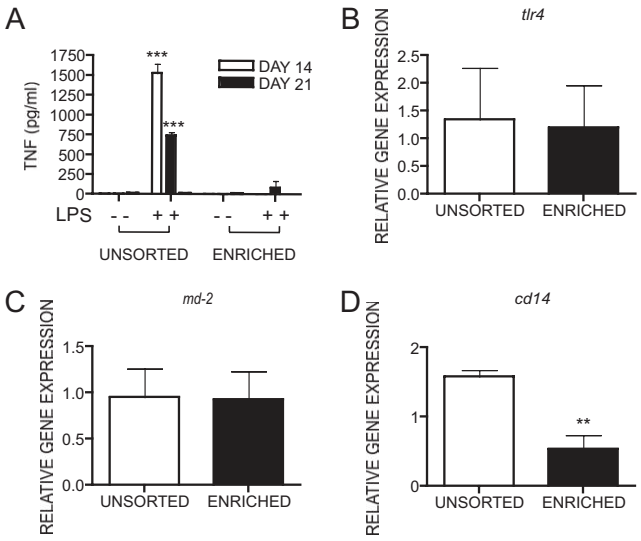

FIGURE 4. Macrophages present in calvarial osteoblast cultures produce TNF upon LPS recognition via the TLR4-CD14 receptor complex. Unsorted and enriched calvarial osteoblasts were treated with 100 ng/ml LPS for 2 h at days 14 and 21. *A,* Secreted TNF protein was quantified by ELISA. Data are mean ± SEM of three replicas within one experiment. Statistical significance (***, $p < 0.001$) was determined by paired *t* test. Data are representative of two independent experiments. Expression of *tlr4* (*B*), *md-2* (*C*), and *cd14* (*D*) in unsorted and enriched osteoblast populations at day 21 were determined by quantitative real-time RT-PCR. Data are mean ± SEM of three biological replicas. Statistical significance (**, $p < 0.01$) was determined by one-way ANOVA.

These observations suggest that either mature osteoblasts and mature macrophages are more closely related than previously supposed or that the osteoblast cell preparations coisolate a population of macrophages. The presence of mature macrophages in primary osteoblast cultures was assessed using immunocytochemistry and flow cytometric analysis. F4/80$^+$ mature macrophages were present throughout the osteoblast differentiation time course (Fig. 2*C*) in conditions where no exogenous CSF-1 (a required macrophage survival factor in vitro) was added. Osteoblasts are known to make CSF-1 to regulate osteoclastogenesis (21); therefore, the primary osteoblasts within these cultures likely produce sufficient CSF-1 to sustain the growth and proliferation of macrophages. Indeed, CSF-1 mRNA is abundant in our calvarial osteoblast cultures (http://symatlas.gnf.org/SymAtlas/and GEO experiment 11339). The number of F4/80$^+$ macrophages in the osteoblast cultures increased over the time course (Fig. 2*C*) and F4/80$^+$ cells with morphological features of mitosis were detected (Fig. 2*D*, arrows), suggesting that macrophage proliferation occurred under these conditions. The expansion of these coisolated macrophages is further supported by the significant increase in gene expression of macrophage markers *csf1r* and *emr1* over the time course (Fig. 2, *A* and *B*). The presence of F4/80$^+$ mature macrophages within the calvarial cultures could be due to either coisolation of a population of tissue macrophages or macrophage differentiation from coisolated myeloid precursors (13). To distinguish between these two possibilities, we assessed whether F4/80$^+$ mature tissue macrophages were present within the freshly isolated calvarial cells via flow cytometric analysis. As shown in Fig. 2*F*, 15.9% of the primary calvarial digest cells expressed F4/80, confirming that a population of mature F4/80$^+$ macrophages was coisolated with primary calvarial osteoblasts. Flow cytometric analysis demonstrated relatively consistent proportions (11.2–16.3%) of F4/80$^+$ macrophages within each digest fraction generated during primary calvarial cell isolation, suggesting that the cells might be colocated

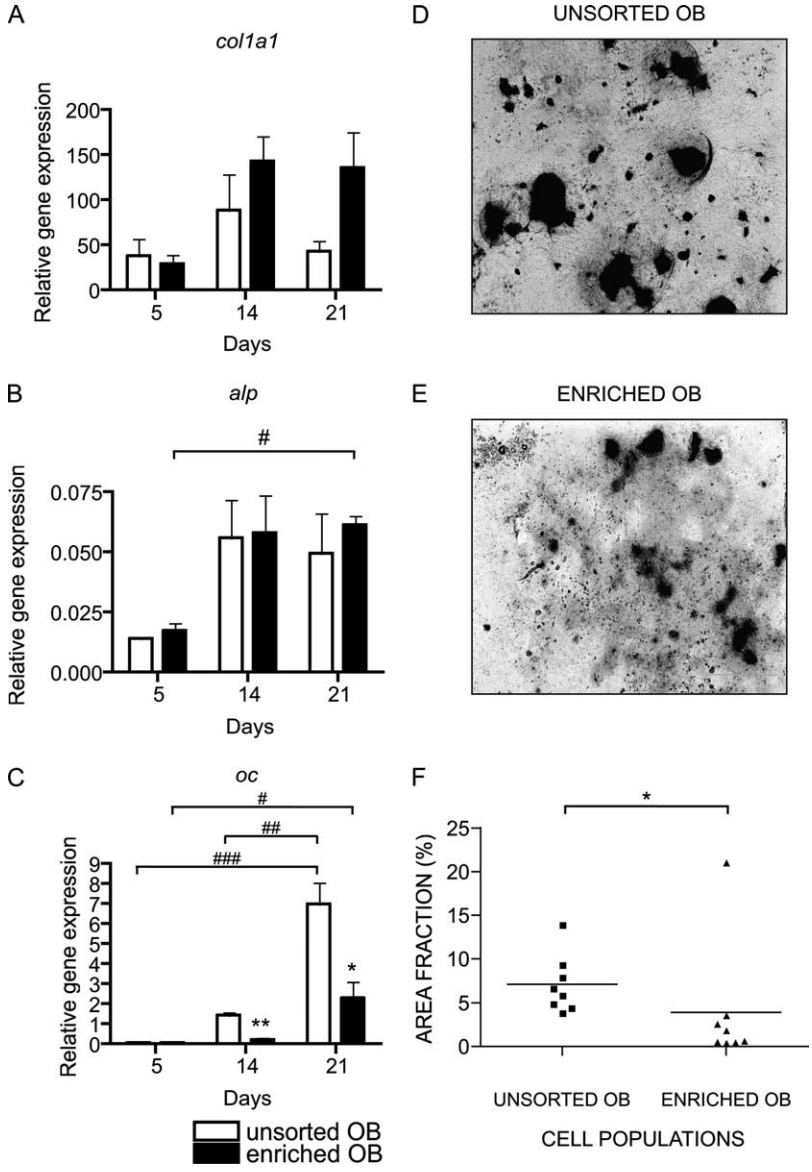

FIGURE 5. Impaired osteoblast mineralization in the absence of macrophages. Real-time RT-PCR quantified the expression of osteoblast markers *col1a1* (*A*), (B) *alp* (*B*), and *oc* (*C*) in unsorted and enriched osteoblast populations throughout a differentiation time course. Data are mean ± SEM of three independent experiments. Statistical significance between populations (*, $p < 0.05$ and **, $p < 0.01$) was determined by unpaired *t* test and significance across the time course was calculated using one-way ANOVA (#, $p < 0.05$; ##, $p < 0.01$; and ###, $p < 0.001$). Osteoblast mineralization was determined by von Kossa staining (black precipitate) in the unsorted osteoblast population (*D*) and the enriched osteoblast population (*E*). Original magnification, ×2. *F,* ImageJ software was used to quantify the area of mineralization. Results were pooled from three independent experiments and analyzed using the Mann-Whitney *t* test (*, $p < 0.05$).

and released simultaneously. This result also indicated that OsteoMacs constitute approximately one-sixth of the total cells within calvarial osteal tissues.

Enrichment of primary osteoblasts

The persistence of mature macrophages in primary osteoblast cultures implies that some cellular functions that have been ascribed to osteoblasts using these preparations as a model system may actually be mediated by the coisolated macrophages or require macrophage-osteoblast interaction. To address this possibility, we developed a procedure to enrich primary osteoblasts, as outlined in *Materials and Methods*. Flow cytometric analysis demonstrated effective removal of F4/80$^+$ macrophages in the enriched osteoblast population (Fig. 3, *A* and *B*). The removal of F4/80$^+$ macrophages and their ongoing absence in standard 21-day osteoblast differentiation experiments was also confirmed using immunocytochemistry (Fig. 3, *C* and *D*). Furthermore, *emr1* mRNA expression was either undetectable or minimal throughout the time course (Fig. 3*E*). These results demonstrate successful depletion of macrophages from primary calvarial osteoblast cultures.

Macrophages are the LPS-responsive cell within primary osteoblast cultures

Previously, primary calvarial osteoblast preparations have been shown to respond to LPS and express the LPS receptor TLR4 (*tlr4*; NM_021297.2) (12). LPS is a major immunostimulatory component of the cell wall of Gram-negative bacteria and potently activates macrophages (22). We examined whether macrophages contribute to the previously reported ability of primary osteoblast cultures to respond to LPS (12). Unsorted and enriched day 14- and day 21-calvarial osteoblast cultures were stimulated with LPS. LPS induction of the proinflammatory cytokine TNF was quantified using ELISA and significant levels of TNF were produced by unsorted osteoblasts at days 14 and 21 (Fig. 4*A*). By contrast, TNF production by enriched osteoblasts was minimal, indicating that depletion of macrophages eliminated the LPS responsiveness of these cultures (Fig. 4*A*). Mature macrophages were also observed in bone explant cultures (data not shown), another common means of obtaining human and rodent primary osteoblasts (23, 24). Immunocytochemical analysis was used to locate TNF and showed that

F4/80$^+$ mature macrophages are the cellular source of TNF within these cultures (data not shown).

We also examined the expression of the receptor complex responsible for LPS recognition (the LPS receptor *tlr4* (25), the accessory molecule *md-2* (NM_016923.1) (26), and coreceptor *cd14* (NM_009841.3) (27)) in unsorted and enriched osteoblast populations. Quantitative real-time RT-PCR demonstrated similar expression levels of *tlr4* (Fig. 4*B*) and *md-2* (Fig. 4*C*) in both unsorted and enriched osteoblasts. However, in keeping with its known myeloid-restricted expression (27), the expression level of *cd14* was greatly reduced in the enriched osteoblast population (Fig. 4*D*). This observation supports that it is the macrophages within the unsorted cells that are the primary source of *cd14* expression. Hence, primary osteoblasts do not express all of the receptor components required for responding to pathophysiological levels of LPS.

Macrophage depletion impairs osteoblast differentiation and mineralization

To investigate possible codependence between macrophages and osteoblasts, we quantitated expression of osteoblast markers in unsorted and enriched calvarial preparations throughout a standard differentiation time course. There was no difference in expression of the early osteoblast differentiation marker genes *col1a1* (Fig. 5*A*) or *alp* (Fig. 5*B*) across the time course. However, expression of the mineralization marker *oc* in day 14- and day 21-enriched osteoblasts was significantly lower than that in unsorted cells (Fig. 5*C*), suggesting that macrophages contribute specifically to osteoblast maturation and mineralization rather than proliferation and differentiation.

To confirm this putative role, we compared osteoblast mineralization in the unsorted and enriched osteoblast cultures. Cell seeding was adjusted so that an equivalent number of osteoblasts was plated in both unsorted and enriched populations. Unsorted and enriched osteoblasts were subjected to standard differentiation conditions and the amount of mineralization was compared between the two populations by von Kossa staining at day 21. Osteoblast enrichment resulted in reduced mineralization (Fig. 5*E*) compared with the unsorted osteoblasts (Fig. 5*D*). This decrease in mineralization was significant, as determined by quantitation of the area of mineral deposition (Fig. 5*F*). The observations confirm that macrophage removal impairs osteoblast mineralization in vitro.

Macrophages are required for osteoblast mineralization in response to elevated extracellular calcium

Extracellular calcium is known to be an important physiological stimulus of bone formation (28) and high extracellular calcium concentrations are a characteristic feature of the bone microenvironment (29). The apparent macrophage contribution to osteoblast mineralization in vitro (Fig. 5) prompted us to investigate more specifically whether macrophages are essential for optimal osteoblast function in response to the physiological stimulus of extracellular calcium. Enriched osteoblasts were cocultured with either bone macrophages or BMMs in 14 mM extracellular calcium for 14 days. Von Kossa staining showed that minimal mineralization occurred in the absence of extracellular calcium in any of the cell combinations (Fig. 6). Minimal mineralization also occurred in enriched osteoblasts cultured without macrophages (Fig. 6*A*). In contrast, extensive mineralization occurred when enriched osteoblasts were cocultured with macrophages (either bone macrophages or BMMs) in the presence of extracellular calcium (Fig. 6*A*). Quantitation of the mineralized area confirmed a significant

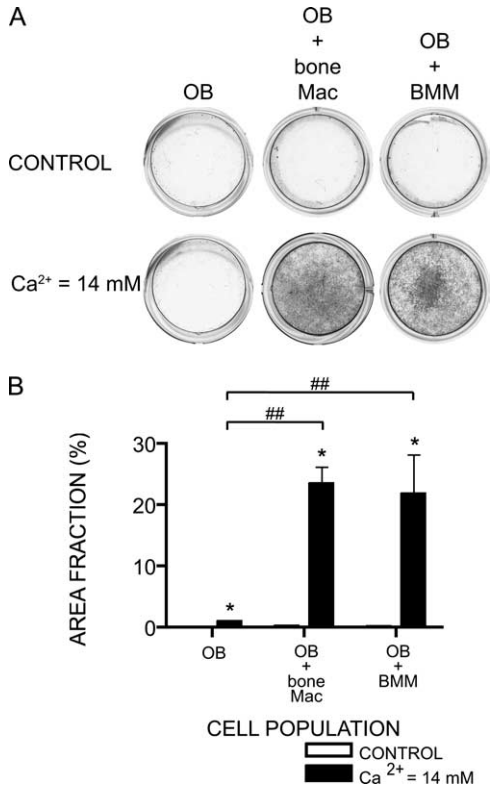

FIGURE 6. Macrophages promote osteoblast (OB) mineralization in response to extracellular calcium in vitro. Enriched calvarial osteoblasts were cocultured with bone macrophages (bone Mac) or BMMs in the presence of 14 mM extracellular calcium for 14 days. *A,* Osteoblast mineralization was determined by von Kossa staining. *B,* Area of mineralization was quantified using ImageJ software. Data are mean ± SEM of three replicas within one experiment. Data are representative of three independent experiments. Statistically significant differences were calculated using paired *t* tests between treatments (*, $p < 0.05$) and one-way ANOVA between cell types (##, $p < 0.01$).

23-fold increase in mineral deposition when macrophages were present (Fig. 6*B*).

OsteoMacs are associated with sites of bone modeling in vivo

If OsteoMacs control bone formation in vivo, we would expect them to be associated with bone forming and mineralizing osteoblasts in situ. Sites of osteoblast-mediated bone modeling can be readily identified by the presence of mature cuboidal osteoblasts lining bone surfaces and verified by demonstrating that these osteoblasts express the bone matrix protein type I collagen (30) and the mineralization marker osteocalcin (31). Immunohistochemical staining for F4/80 in sagittal long bone sections from 4-wk-old rapidly growing mice showed that F4/80$^+$ OsteoMacs formed a distinctive canopy-like structure over cuboidal osteoblast-like cells on bone surfaces (Fig. 7*A*). This cellular distribution was more striking on the endosteal surface (Fig. 7*A*) but was also observed in periosteum (data not shown). This most likely reflects difficulty in visualizing the more complex three-dimensional structure of the periosteum in a two-dimensional section. We observed F4/80$^+$ cell processes forming contacts with the underlying osteoblast-like cell layer (Fig. 7, *A* and *B*, arrows). Staining for F4/80 and osteoblast markers in serial sections demonstrated that the F4/80$^+$ OsteoMacs (Fig. 7*B*) juxtaposed cuboidal osteocalcin$^+$ (Fig. 7*C*) and collagen type I$^+$ (Fig. 7*D*) mature osteoblasts. Using adapted histomorphometic analysis, we determined that 77 ± 2.1% ($n = 7$) of

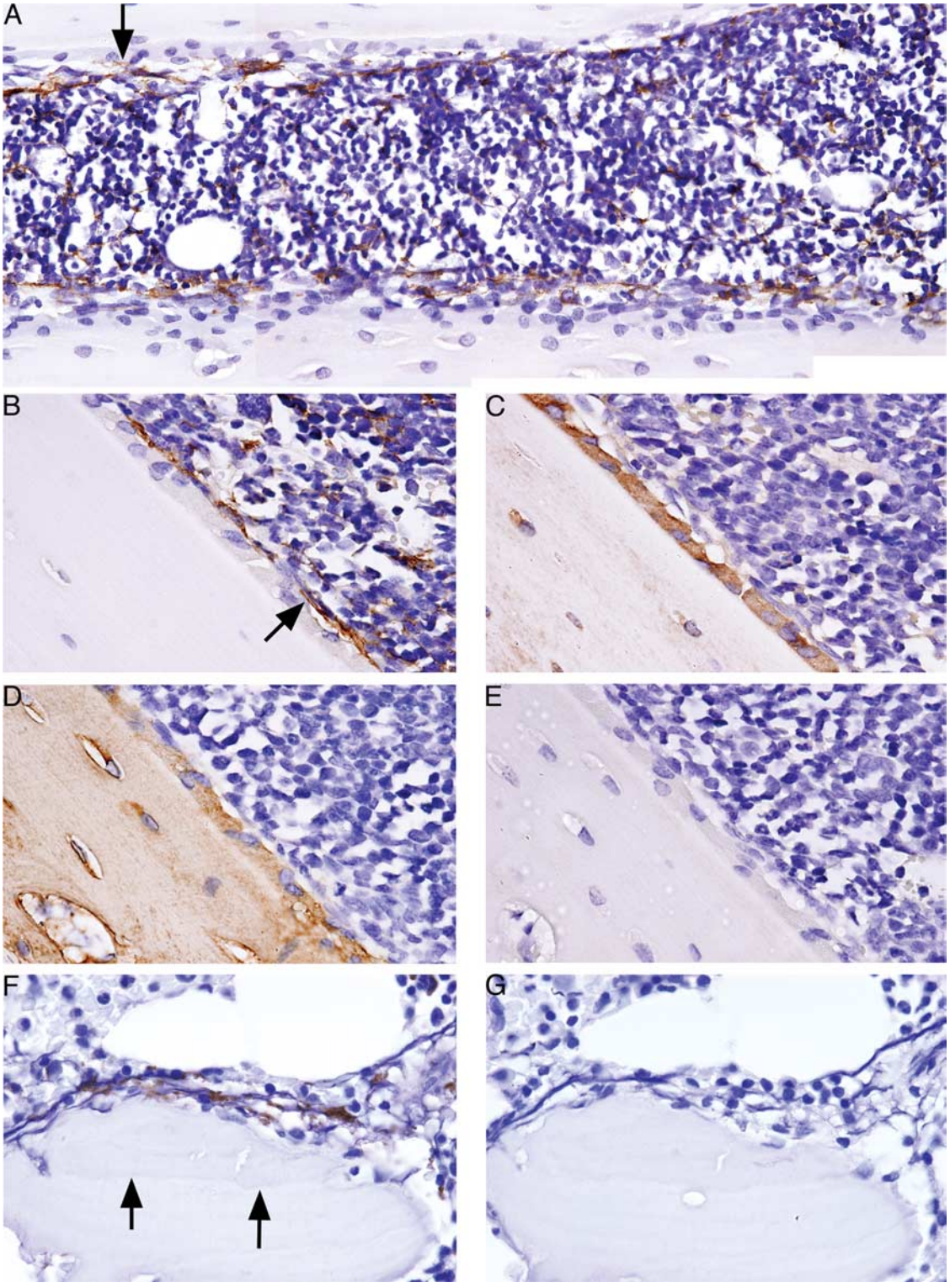

FIGURE 7. OsteoMacs form a canopy structure over mature osteoblasts at sites of bone formation. *A–E,* Immunohistochemical staining for F4/80 and mature osteoblast markers at sites of endosteal bone apposition in 4-wk-old murine long bone in the diaphyseal region. All sections were counterstained with hematoxylin. *A,* Tiled image generated from three overlapping digital micrographs of F4/80 staining (brown). The image illustrates the presence of a F4/80$^+$ OsteoMac canopy structure over cuboidal mature osteoblast-like cells on opposing endosteal surfaces. *B–E,* Serial sections of the same anatomical region: *B,* F4/80 staining demonstrating the F4/80$^+$ OsteoMac canopy structure over cuboidal mature osteoblasts expressing osteocalcin (*C*, brown) and collagen type I (*D*, brown). *E,* An isotype control Ab for anti-osteocalcin and anti-collagen type I Abs confirmed specificity of staining. Images are representative of seven mice. *F* and *G,* Immunohistochemistry for the macrophage marker CD68 in OA human bone tissue. *F,* Staining for CD68 (brown) demonstrated the presence of a CD68$^+$ canopy-like cell structure in the bone microenvironment. Basophilic collagen lines (arrow, stained deeper blue with hematoxylin) were evident within the underlying bone, suggesting recent bone formation. *G,* The specificity of staining was confirmed using the relevant isotype control Ab in a serial section. Original magnifications: ×60 (*A*) and ×100 (*B–G*).

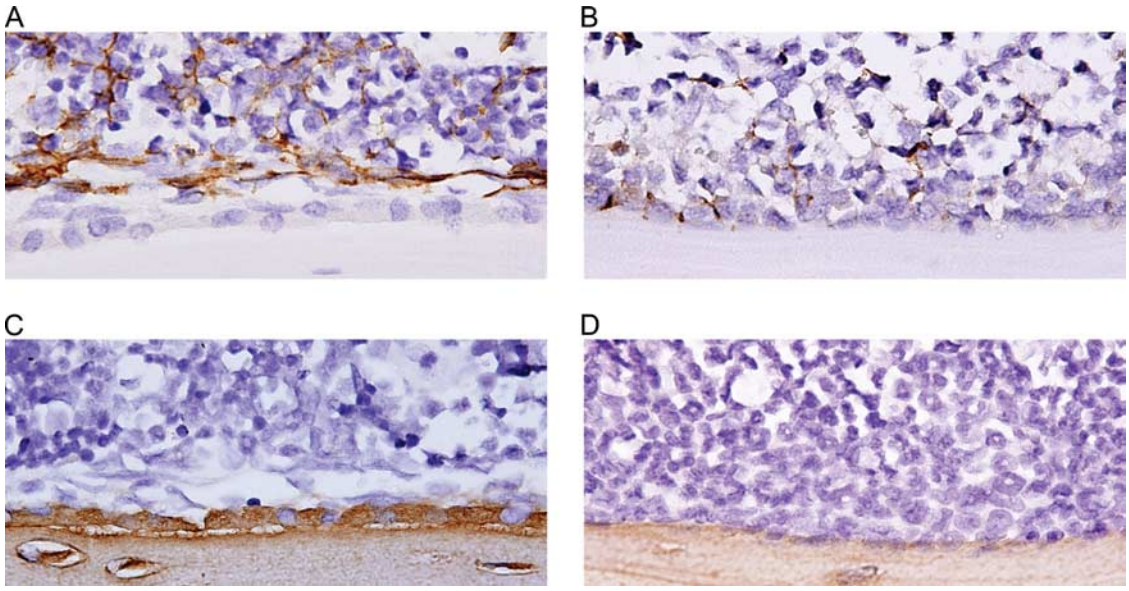

FIGURE 8. Systemic macrophage depletion results in complete loss of mature osteoblast bone-forming surface. Conditional macrophage depletion was achieved in MAFIA mice upon treatment with AP20187 ligand. Immunohistochemical staining for F4/80 and collagen type I in sagittal cross-sections of cortical long bones demonstrated the presence of F4/80$^+$ OsteoMac canopy structure (*A*) over cuboidal mature osteoblasts (*C*) at a site of bone modeling in vehicle-treated mice and the absence of F4/80$^+$ OsteoMac canopy structure (*B*) and osteoblast bone surface in ligand-treated mice (*D*). Relative paucity of F4/80$^+$ macrophages within the bone marrow in ligand-treated animals (*B*) is evident on comparison with vehicle-treated controls (*A*). Specificity of staining was confirmed by matched isotype control staining in serial sections (data not shown). Sections were counterstained with hematoxylin. Original magnification, ×60. Images are representative of seven mice.

the endosteal mature osteoblast surface (ObS) in the diaphyseal cortical modeling zone of young mice was covered by the F4/80$^+$ OsteoMac canopy. This anatomical distribution was also present at modeling surfaces in older mice (10 wk and 6 mo). Trabecular bone sections from human OA bone stained for the macrophage marker CD68 identified OsteoMacs associated with areas of recent bone formation (Fig. 7*F*). The close proximity between OsteoMacs and osteoblasts in situ and their assembly into an organized structure suggest that OsteoMacs participate in osteoblast-mediated bone formation in vivo.

The role of macrophages in maintenance of mature osteoblast bone modeling surface in vivo

To more directly assess the importance of OsteoMacs in osteoblast function in vivo, we used the MAFIA mouse model, in which the *csf1r* promoter directs expression of a ligand-inducible Fas-based suicide receptor to cells of the mononuclear phagocyte lineage (16). Flow cytometric analysis of bone marrow collected from the contralateral limb of each animal at the time of harvest confirmed that F4/80$^+$ macrophage depletion was achieved in all animals, with an average reduction of 52.4% in ligand-treated mice compared with control mice. Representative images of F4/80$^+$ macrophage depletion in the bone marrow are shown in Fig. 8, *A* and *B*. Maintenance of the osteoblast surface was examined on endosteal bone surfaces in a region of bone modeling, which was confirmed by the presence of mature osteoblasts (Fig. 8*C*), F4/80$^+$ OsteoMac canopy (Fig. 8*A*), and an absence of TRAP$^+$ osteoclasts within the immediate environment (data not shown). Adapted histomorphometric analysis on seven vehicle-treated and seven ligand-treated MAFIA mice showed that vehicle- treated animals had 68.8 ± 3.4% osteoblast bone surface and that 64.5 ± 6.7% of this was covered by an OsteoMac canopy. By contrast, the ligand-treated mice had 0% osteoblast bone surface and subsequently no OsteoMac canopy. Representative images are shown in Fig. 8, *B* and *D*. This observation supports that disruption of OsteoMac number and distribution has a rapid and detrimental effect on the maintenance of osteoblast bone modeling surface.

Discussion

The relatively new concept of osteoimmunology describes the complex regulatory interactions between bone and immune cells (32). The intimate relationship between these two systems has been primarily demonstrated in pathological conditions. Macrophages were recognized during fracture repair (33), arteriole calcification (34), and at sites of osteophyte formation in OA animal models (35). Additionally, macrophages were found at sites of pathological bone destruction (36) and contributed to systemic mechanisms in an animal model of osteoporosis (37). We have previously reported the presence of mature tissue macrophages closely associated with bone (6). It is also known that macrophages can express and secrete osteoactive cytokines (35), matrix metalloproteinases (36), and bone morphogenetic proteins (35).

In the current study, we confirmed that macrophages are an integral component of mouse and human osteal tissues in vivo and that they represent a discreet resident macrophage population that we have termed OsteoMacs. This observation is surprising but not entirely unexpected, since macrophages are a resident population in most body tissues (3). We also demonstrated that F4/80$^+$ mature tissue macrophages are a significant component of primary osteoblast cultures generated by both calvarial digestion and bone explant methods. Their maintenance and proliferation within these cultures was likely sustained by osteoblast production of CSF-1, as supported by our microarray data (http://symatlas.gnf.org/SymAtlas/and GEO experiment 11339) and extensive literature including Mundy et al. (21). Given that other resident macrophage populations have important tissue-specific functions (4), we investigated the potential bone-specific functions of OsteoMacs in the osteal microenvironment.

We first determined whether immune-related functions that were attributed to osteoblasts using primary cultures as the model system (11, 12) may in fact be mediated by the coisolated macrophages and provided evidence supporting that this is the case for LPS responsiveness. Osteoblast cell lines have been reported to be LPS responsive but the concentration of LPS used was very high (12). Indeed, our microarray and quantitative real-time PCR data showed that osteoblasts do express both *tlr4* and *md-2*. However, they expressed minimal levels of *cd14*, a coreceptor that increases cellular sensitivity to LPS and is required for responding to pathophysiological concentrations of LPS (27). The *cd14* expression in the enriched osteoblasts could also be attributed to the small residual population of *emr1*-expressing macrophages at day 21. High expression of TLR4 and MD-2 by osteoblasts does raise the possibility that there is an alternative endogenous TLR4 ligand. The expression of TLR4 and MD-2 on osteoblasts would enable these cells to respond to high doses of LPS in vitro. However, it is unlikely that osteoblasts can respond to doses of LPS that would be encountered in vivo. Our current observations indicate that OsteoMacs are the in vivo LPS-responsive cell within osteal tissues. It is clear that osteoblast functional abilities inferred solely from primary osteoblast preparations need to be reassessed to determine whether macrophages significantly contributed to the experimental findings.

To determine whether OsteoMacs can regulate osteoblast function, we compared osteoblast gene expression and function between unsorted (macrophage-containing) and enriched (macrophage-depleted) primary osteoblast populations in standard in vitro differentiation assays that use β-glycerol phosphate plus ascorbic acid to induce osteoblast differentiation and function. We observed no significant differences in the expression of early differentiation markers, indicating that macrophages are not required for early osteoblast differentiation. In contrast, *oc* mRNA expression and overall mineralization was significantly reduced in enriched osteoblasts when compared with unsorted cells, demonstrating a failure in terminal osteoblast maturation in the absence of macrophages.

Bone remodeling is a highly orchestrated multicellular process that requires the sequential and balanced events of osteoclast-mediated bone resorption and osteoblast-mediated bone formation (38). The spatial and temporal relationships between these cells are maintained throughout the remodeling process (39). A canopy structure over sites of bone remodeling was previously reported in human tissue (40, 41). These canopy cells, proposed to be bone lining cells (41) or preosteoblasts (40), were postulated to create an enclosed compartment for local communication and coordination during this complex physiological process (39). In contrast to bone remodeling, bone modeling is an anabolic process that does not comprise the tight coupling of bone resorption to bone formation (17). We report for the first time that a distinctive canopy structure primarily consisting of OsteoMacs is formed over bone-forming osteoblasts at sites of bone modeling. The relative absence of $TRAP^+$ multinuclear osteoclasts within the immediate environment confirmed that the process being examined here was a bone-modeling event, not remodeling, and therefore is independent of osteoclast function. The bone-modeling canopy cell identity and functional importance was strongly supported by the impact of partial macrophage depletion in the MAFIA mouse on the macrophage canopy architecture, osteoblast bone surface, and endosteal niche. Given the close relationship between macrophages and osteoclasts, OsteoMacs within the canopy at sites of bone modeling may simulate the coupling process that is proposed to occur between osteoclasts and osteoblasts in bone remodeling (38).

We next demonstrated that macrophages are essential for osteoblast mineralization in response to the physiological proanabolic stimulus of elevated extracellular calcium (28). We demonstrated that both OsteoMacs and BMM were able to promote osteoblast mineralization in response to this stimulus. This suggests that exposure of in vitro-generated macrophages to the appropriate environmental conditions results in their adaptation to an OsteoMac-like phenotype. Given that a salient feature of macrophages is their ability to rapidly adapt and respond to environment cues, this is not an unexpected outcome (3, 4). Macrophage enhancement of vascular calcification in vitro has been previously reported (42), providing some precedence for macrophage direction of mineral deposition. Macrophages have also been shown by others to produce osteoinductive factors such as TGF-β (43), osteopontin (44), 1,25-dihydroxyvitamin D_3 (45), and bone morphogenetic protein 2 (46) under various conditions. The overall regulatory effect of macrophages on osteoblast function is likely to be mediated by a combination of factors. Given that osteoblasts also express the calcium-sensing receptor CaR (47), it is possible that bidirectional cellular communication between macrophages and osteoblasts drives mineralization. The results generated using the two osteoblast differentiation culture systems here are consistent with the concept that macrophages participate in osteoblast mineralization, but that the degree of contribution in vitro spans from enhancement (β-glycerol phosphate plus ascorbic acid) to required (elevated extracellular calcium), depending on the stimulus encountered.

An obvious line of inquiry that we are actively investigating is whether the OsteoMac population is capable of participating in osteoclastogenesis, either directly or indirectly. As both macrophages and osteoclasts develop from hematopoietic precursors along the myeloid lineage (48) and some macrophage populations can differentiate into osteoclasts in vitro (49), one candidate functional role for OsteoMacs is as an immediate in vivo osteoclast precursor. It must be emphasized that, although the two cell populations are related by their shared precursors and CSF-1 dependence, the OsteoMacs are not osteoclasts, as the F4/80 Ag is completely absent from osteoclasts (5). A more likely scenario is that OsteoMacs activated by proinflammatory stimuli including LPS (as in Fig. 4*A*) produce pro-osteoclastogenic cytokines such as TNF (50, 51), IL-6 (52, 53), and IL-1 (50, 54) and could potentially promote osteoclast differentiation and/or function. As such, OsteoMacs may provide a candidate cellular mechanism to explain why chronic inflammation (55) and systemic infection (56) often result in osteopenia/osteoporosis. Based upon their apposition to bone surfaces and their well-known ability to detect dying cells (57), OsteoMacs are also the most obvious candidates to detect and respond to bone damage (e.g., apoptotic death of osteoblasts and osteocytes), a critical event in initiation of bone remodeling and osteoclast recruitment (58).

The trophic roles of tissue macrophages are being appreciated in many other organ systems (7). For example, resident and recruited macrophages have been shown to control survival, degeneration, and replacement of olfactory sensory neurons, another system in which turnover is highly regulated (59). Our data show that OsteoMacs, like macrophages in many other organs (4), occupy a precise anatomical niche and that they are integral to maintenance of osteal tissue homeostasis. Because macrophages have evolved to detect and respond to subtle changes in their local environment (4), we propose that OsteoMacs serve as sentinel cells in osteal tissues and in response to unique local stimuli, regulate osteoblast function, and subsequently bone dynamics.

Acknowledgments

We thank Prof. Don Cohen for the MAFIA mice; Dr. Andrew Su and Dr. John Walker for contribution to the Symatlas microarray project at the Genomics Institute of the Novartis Research Foundation; Prof. Jenny Stow for providing the TNF Ab; and Ekaterina Bogatyreva, Queensland Brain Institute FACS facility and Institute for Molecular Bioscience Animal House for technical assistance. We also thank Profs. Steven Goldring and Gregory Mundy for constructively critiquing this manuscript. Confocal microscopy was performed at the Australian Research Foundation/Institute for Molecular Bioscience Dynamic Imaging Facility for Cancer Biology, which was established with the support of the Australian Cancer Research Foundation.

Disclosures

The authors have no financial conflict of interest.

References

1. Stein, G. S., J. B. Lian, and T. A. Owen. 1990. Relationship of cell growth to the regulation of tissue-specific gene expression during osteoblast differentiation. *FASEB J.* 4: 3111–3123.
2. Teitelbaum, S. L. 2007. Osteoclasts: what do they do and how do they do it? *Am. J. Pathol.* 170: 427–435.
3. Gordon, S., and P. R. Taylor. 2005. Monocyte and macrophage heterogeneity. *Nat. Rev. Immunol.* 5: 953–964.
4. Hume, D. A. 2006. The mononuclear phagocyte system. *Curr. Opin. Immunol.* 18: 49–53.
5. Gordon, S. 1995. The macrophage. *BioEssays* 17: 977–986.
6. Hume, D. A., J. F. Loutit, and S. Gordon. 1984. The mononuclear phagocyte system of the mouse defined by immunohistochemical localization of antigen F4/80: macrophages of bone and associated connective tissue. *J. Cell Sci.* 66: 189–194.
7. Rae, F., K. Woods, T. Sasmono, N. Campanale, D. Taylor, D. A. Ovchinnikov, S. M. Grimmond, D. A. Hume, S. D. Ricardo, and M. H. Little. 2007. Characterisation and trophic functions of murine embryonic macrophages based upon the use of a Csf1r-EGFP transgene reporter. *Dev. Biol.* 308: 232–246.
8. Michelangeli, V. P., A. E. Fletcher, E. H. Allan, G. C. Nicholson, and T. J. Martin. 1989. Effects of calcitonin gene-related peptide on cyclic AMP formation in chicken, rat, and mouse bone cells. *J. Bone Miner. Res.* 4: 269–272.
9. Owen, T. A., M. Aronow, V. Shalhoub, L. M. Barone, L. Wilming, M. S. Tassinari, M. B. Kennedy, S. Pockwinse, J. B. Lian, and G. S. Stein. 1990. Progressive development of the rat osteoblast phenotype in vitro: reciprocal relationships in expression of genes associated with osteoblast proliferation and differentiation during formation of the bone extracellular matrix. *J. Cell. Physiol.* 143: 420–430.
10. Wong, G. L., and D. V. Cohn. 1975. Target cells in bone for parathormone and calcitonin are different: enrichment for each cell type by sequential digestion of mouse calvaria and selective adhesion to polymeric surfaces. *Proc. Natl. Acad. Sci. USA* 72: 3167–3171.
11. Ruiz, C., E. Perez, M. Vallecillo-Capilla, and C. Reyes-Botella. 2003. Phagocytosis and allogeneic T cell stimulation by cultured human osteoblast-like cells. *Cell. Physiol. Biochem.* 13: 309–314.
12. Kikuchi, T., T. Matsuguchi, N. Tsuboi, A. Mitani, S. Tanaka, M. Matsuoka, G. Yamamoto, T. Hishikawa, T. Noguchi, and Y. Yoshikai. 2001. Gene expression of osteoclast differentiation factor is induced by lipopolysaccharide in mouse osteoblasts via Toll-like receptors. *J. Immunol.* 166: 3574–3579.
13. Pascual, C. J., P. R. Sanberg, W. Chamizo, S. Haraguchi, D. Lerner, M. Baldwin, and N. S. El-Badri. 2005. Ovarian monocyte progenitor cells: phenotypic and functional characterization. *Stem Cells Dev.* 14: 173–180.
14. Sasmono, R. T., D. Oceandy, J. W. Pollard, W. Tong, P. Pavli, B. J. Wainwright, M. C. Ostrowski, S. R. Himes, and D. A. Hume. 2003. A macrophage colony-stimulating factor receptor-green fluorescent protein transgene is expressed throughout the mononuclear phagocyte system of the mouse. *Blood* 101: 1155–1163.
15. Ripoll, V. M., K. M. Irvine, T. Ravasi, M. J. Sweet, and D. A. Hume. 2007. Gpnmb is induced in macrophages by IFN-γ and lipopolysaccharide and acts as a feedback regulator of proinflammatory responses. *J. Immunol.* 178: 6557–6566.
16. Burnett, S. H., B. J. Beus, R. Avdiushko, J. Qualls, A. M. Kaplan, and D. A. Cohen. 2006. Development of peritoneal adhesions in macrophage depleted mice. *J. Surg. Res.* 131: 296–301.
17. Dempster, D. W. 2006. Anatomy and functions of the adult skeleton. In *Primer on the Metabolic Bone Diseases and Disorders of Mineral Metabolism*, 6th Ed. J. F. Murray, ed. American Society for Bone and Mineral Research, Washington, DC, pp. 7–11.
18. Holness, C. L., and D. L. Simmons. 1993. Molecular cloning of CD68, a human macrophage marker related to lysosomal glycoproteins. *Blood* 81: 1607–1613.
19. Su, A. I., T. Wiltshire, S. Batalov, H. Lapp, K. A. Ching, D. Block, J. Zhang, R. Soden, M. Hayakawa, G. Kreiman, et al. 2004. A gene atlas of the mouse and human protein-encoding transcriptomes. *Proc. Natl. Acad. Sci. USA* 101: 6062–6067.
20. Hume, D. A., I. L. Ross, S. R. Himes, R. T. Sasmono, C. A. Wells, and T. Ravasi. 2002. The mononuclear phagocyte system revisited. *J. Leukocyte Biol.* 72: 621–627.
21. Mundy, G. R., D. Chen, and B. O. Oyajobi. 2003. Bone remodeling. In *Primer on the Metabolic Bone Diseases and Disorders of Mineral Metabolism*, 5th Ed. J. F. Murray, ed. American Society for Bone and Mineral Research, Washington, DC, pp. 46–58.
22. Sweet, M. J., and D. A. Hume. 1996. Endotoxin signal transduction in macrophages. *J. Leukocyte Biol.* 60: 8–26.
23. Gronthos, S., A. C. Zannettino, S. E. Graves, S. Ohta, S. J. Hay, and P. J. Simmons. 1999. Differential cell surface expression of the STRO-1 and alkaline phosphatase antigens on discrete developmental stages in primary cultures of human bone cells. *J. Bone Miner Res.* 14: 47–56.
24. Guo, Z., H. Li, X. Li, X. Yu, H. Wang, P. Tang, and N. Mao. 2006. In vitro characteristics and in vivo immunosuppressive activity of compact bone-derived murine mesenchymal progenitor cells. *Stem Cells* 24: 992–1000.
25. Poltorak, A., X. He, I. Smirnova, M. Y. Liu, C. Van Huffel, X. Du, D. Birdwell, E. Alejos, M. Silva, C. Galanos, et al. 1998. Defective LPS signaling in C3H/HeJ and C57BL/10ScCr mice: mutations in Tlr4 gene. *Science* 282: 2085–2088.
26. Schromm, A. B., E. Lien, P. Henneke, J. C. Chow, A. Yoshimura, H. Heine, E. Latz, B. G. Monks, D. A. Schwartz, K. Miyake, and D. T. Golenbock. 2001. Molecular genetic analysis of an endotoxin nonresponder mutant cell line: a point mutation in a conserved region of MD-2 abolishes endotoxin-induced signaling. *J. Exp. Med.* 194: 79–88.
27. Wright, S. D., R. A. Ramos, P. S. Tobias, R. J. Ulevitch, and J. C. Mathison. 1990. CD14, a receptor for complexes of lipopolysaccharide (LPS) and LPS binding protein. *Science* 249: 1431–1433.
28. Dvorak, M. M., A. Siddiqua, D. T. Ward, D. H. Carter, S. L. Dallas, E. F. Nemeth, and D. Riccardi. 2004. Physiological changes in extracellular calcium concentration directly control osteoblast function in the absence of calciotropic hormones. *Proc. Natl. Acad. Sci. USA* 101: 5140–5145.
29. Adams, G. B., K. T. Chabner, I. R. Alley, D. P. Olson, Z. M. Szczepiorkowski, M. C. Poznansky, C. H. Kos, M. R. Pollak, E. M. Brown, and D. T. Scadden. 2006. Stem cell engraftment at the endosteal niche is specified by the calcium-sensing receptor. *Nature* 439: 599–603.
30. Nefussi, J. R., M. L. Boy-Lefevre, H. Boulekbache, and N. Forest. 1985. Mineralization in vitro of matrix formed by osteoblasts isolated by collagenase digestion. *Differentiation* 29: 160–168.
31. de Pollak, C., E. Arnaud, D. Renier, and P. J. Marie. 1997. Age-related changes in bone formation, osteoblastic cell proliferation, and differentiation during postnatal osteogenesis in human calvaria. *J. Cell. Biochem.* 64: 128–139.
32. Arron, J. R., and Y. Choi. 2000. Bone versus immune system. *Nature* 408: 535–536.
33. Andrew, J. G., S. M. Andrew, A. J. Freemont, and D. R. Marsh. 1994. Inflammatory cells in normal human fracture healing. *Acta Orthop. Scand.* 65: 462–466.
34. Smith, J. D., E. Trogan, M. Ginsberg, C. Grigaux, J. Tian, and M. Miyata. 1995. Decreased atherosclerosis in mice deficient in both macrophage colony-stimulating factor (*op*) and apolipoprotein E. *Proc. Natl. Acad. Sci. USA* 92: 8264–8268.
35. Blom, A. B., P. L. van Lent, A. E. Holthuysen, P. M. van der Kraan, J. Roth, N. van Rooijen, and W. B. van den Berg. 2004. Synovial lining macrophages mediate osteophyte formation during experimental osteoarthritis. *Osteoarthr. Cartil.* 12: 627–635.
36. Kaneko, M., T. Tomita, T. Nakase, Y. Ohsawa, H. Seki, E. Takeuchi, H. Takano, K. Shi, K. Takahi, E. Kominami, et al. 2001. Expression of proteinases and inflammatory cytokines in subchondral bone regions in the destructive joint of rheumatoid arthritis. *Rheumatology* 40: 247–255.
37. Cenci, S., M. N. Weitzmann, C. Roggia, N. Namba, D. Novack, J. Woodring, and R. Pacifici. 2000. Estrogen deficiency induces bone loss by enhancing T-cell production of TNF-α. *J. Clin. Invest.* 106: 1229–1237.
38. Martin, T. J., and N. A. Sims. 2005. Osteoclast-derived activity in the coupling of bone formation to resorption. *Trends Mol. Med.* 11: 76–81.
39. Parfitt, A. M. 2001. The bone remodeling compartment: a circulatory function for bone lining cells. *J. Bone Miner Res.* 16: 1583–1585.
40. Hauge, E. M., D. Qvesel, E. F. Eriksen, L. Mosekilde, and F. Melsen. 2001. Cancellous bone remodeling occurs in specialized compartments lined by cells expressing osteoblastic markers. *J. Bone Miner Res.* 16: 1575–1582.
41. Rasmussen, H., and P. Bordier. 1974. *Bone Remodeling and Its Relationship to Metabolic Bone Diseases.* William & Wilkins, Baltimore.
42. Tintut, Y., J. Patel, M. Territo, T. Saini, F. Parhami, and L. L. Demer. 2002. Monocyte/macrophage regulation of vascular calcification in vitro. *Circulation* 105: 650–655.
43. Wahl, S. M., N. McCartney-Francis, J. B. Allen, E. B. Dougherty, and S. F. Dougherty. 1990. Macrophage production of TGF-β and regulation by TGF-β. *Ann. NY Acad. Sci.* 593: 188–196.
44. Takahashi, F., K. Takahashi, K. Shimizu, R. Cui, N. Tada, H. Takahashi, S. Soma, M. Yoshioka, and Y. Fukuchi. 2004. Osteopontin is strongly expressed by alveolar macrophages in the lungs of acute respiratory distress syndrome. *Lung* 182: 173–185.
45. Kreutz, M., R. Andreesen, S. W. Krause, A. Szabo, E. Ritz, and H. Reichel. 1993. 1,25-dihydroxyvitamin D_3 production and vitamin D_3 receptor expression are developmentally regulated during differentiation of human monocytes into macrophages. *Blood* 82: 1300–1307.
46. Honda, Y., T. Anada, S. Kamakura, M. Nakamura, S. Sugawara, and O. Suzuki. 2006. Elevated extracellular calcium stimulates secretion of bone morphogenetic protein 2 by a macrophage cell line. *Biochem. Biophys. Res. Commun.* 345: 1155–1160.
47. Chattopadhyay, N., S. Yano, J. Tfelt-Hansen, P. Rooney, D. Kanuparthi, S. Bandyopadhyay, X. Ren, E. Terwilliger, and E. M. Brown. 2004. Mitogenic action of calcium-sensing receptor on rat calvarial osteoblasts. [Published erratum appears in 2005 *Endocrinology* 146: 3025] *Endocrinology* 145: 3451–3462.

48. Lean, J. M., K. Matsuo, S. W. Fox, K. Fuller, F. M. Gibson, G. Draycott, M. R. Wani, K. E. Bayley, B. R. Wong, Y. Choi, et al. 2000. Osteoclast lineage commitment of bone marrow precursors through expression of membrane-bound TRANCE. *Bone* 27: 29–40.
49. Takeshita, S., K. Kaji, and A. Kudo. 2000. Identification and characterization of the new osteoclast progenitor with macrophage phenotypes being able to differentiate into mature osteoclasts. *J. Bone Miner. Res.* 15: 1477–1488.
50. Stacey, K. J., M. J. Sweet, and D. A. Hume. 1996. Macrophages ingest and are activated by bacterial DNA. *J. Immunol.* 157: 2116–2122.
51. Kobayashi, K., N. Takahashi, E. Jimi, N. Udagawa, M. Takami, S. Kotake, N. Nakagawa, M. Kinosaki, K. Yamaguchi, N. Shima, et al. 2000. Tumor necrosis factor α stimulates osteoclast differentiation by a mechanism independent of the ODF/RANKL-RANK interaction. *J. Exp. Med.* 191: 275–286.
52. Lipford, G. B., T. Sparwasser, M. Bauer, S. Zimmermann, E. S. Koch, K. Heeg, and H. Wagner. 1997. Immunostimulatory DNA: sequence-dependent production of potentially harmful or useful cytokines. *Eur. J. Immunol.* 27: 3420–3426.
53. Sparwasser, T., T. Miethke, G. Lipford, A. Erdmann, H. Hacker, K. Heeg, and H. Wagner. 1997. Macrophages sense pathogens via DNA motifs: induction of tumor necrosis factor-α-mediated shock. *Eur. J. Immunol.* 27: 1671–1679.
54. Jimi, E., I. Nakamura, L. T. Duong, T. Ikebe, N. Takahashi, G. A. Rodan, and T. Suda. 1999. Interleukin 1 induces multinucleation and bone-resorbing activity of osteoclasts in the absence of osteoblasts/stromal cells. *Exp. Cell Res.* 247: 84–93.
55. Walther, F., C. Fusch, M. Radke, S. Beckert, and A. Findeisen. 2006. Osteoporosis in pediatric patients suffering from chronic inflammatory bowel disease with and without steroid treatment. *J. Pediatr. Gastroenterol. Nutr.* 43: 42–51.
56. Bongiovanni, M., and C. Tincati. 2006. Bone diseases associated with human immunodeficiency virus infection: pathogenesis, risk factors and clinical management. *Curr. Mol. Med.* 6: 395–400.
57. Henson, P. M., and D. A. Hume. 2006. Apoptotic cell removal in development and tissue homeostasis. *Trends Immunol.* 27: 244–250.
58. Jilka, R. L., R. S. Weinstein, A. M. Parfitt, and S. C. Manolagas. 2007. Quantifying osteoblast and osteocyte apoptosis: challenges and rewards. *J. Bone Miner. Res.* 22: 1492–1501.
59. Borders, A. S., M. L. Getchell, J. T. Etscheidt, N. van Rooijen, D. A. Cohen, and T. V. Getchell. 2007. Macrophage depletion in the murine olfactory epithelium leads to increased neuronal death and decreased neurogenesis. *J. Comp. Neurol.* 501: 206–218.